Scripta Materialia 145 (2018) 50–53

Contents lists available at ScienceDirect

Scripta Materialia

journal homepage: www.elsevier.com/locate/scriptamat

Regular article

X-ray photoelectron spectroscopy analysis as a tool to assess factors influencing magnetic anisotropy type in Co/MgO system with gold interlayer

Iraida N. Demchenko [a,*], Yevgen Syryanyy [a], Yevgen Melikhov [b], Laurent Nittler [a], Leszek Gladczuk [a], Kinga Lasek [a], Luca Cozzarini [c], Matteo Dalmiglio [c], Andrea Goldoni [c], Pavlo Konstantynov [a], Maryna Chernyshova [d]

[a] Institute of Physics, Polish Academy of Sciences, aleja Lotnikow 32/46, PL-02-668 Warsaw, Poland
[b] School of Engineering, Cardiff University, Newport Rd., Cardiff, CF24 3AA, UK
[c] Elettra-Sincrotrone Trieste S.C.p.A., Strada Statale 14, Basovizza, Trieste, Italy
[d] Institute of Plasma Physics and Laser Microfusion, 23 Hery Str., Warsaw, Poland

ARTICLE INFO

Article history:
Received 8 June 2017
Received in revised form 5 October 2017
Accepted 6 October 2017
Available online 16 October 2017

ABSTRACT

X-ray photoelectron spectroscopy (XPS) studies of Au/Co/Au(0.3 nm)/MgO and Au/Co/MgO systems were conducted in order to monitor the electronic structure modification at Co/MgO interface with/without gold interlayer. A detailed analysis of Co 2*p* states revealed that the amount of minor oxygen contribution at Co/MgO interface decreased after the Au interlayer was added. The obtained XPS results together with density functional theory (DFT) allowed explanation of the increase of surface anisotropy energy in the sample with the gold interlayer in terms of (i) noble and transitional metal *d*-*d* orbital hybridization; (ii) interfacial Co 3*d* and O 2*p*; and (iii) interface imperfection.

A phenomenon of perpendicular magnetic anisotropy (PMA) in Co films combined with Pd, Pt, Au multilayers [1] has opened an exciting field of research inquiring the fundamental origin of PMA and a role of interfacial orbital hybridization [2,3]. Other systems where PMA is noticed are systems based on F/MO_x interfaces, where F represents a ferromagnetic metal, M stands for a diamagnetic metal, and MO_x marks a nonmagnetic oxide (i.e., isolator). The PMA appears when the interface anisotropy energy overcomes the magnetostatic and volume energy contributions to the free energy of the magnetic layer. This type of magnetic anisotropy, a so-called interface or surface anisotropy, was predicted already in 1954 by Néel and is a result of lowering symmetry at the surface or interface. Up to now, many PMA materials have been advanced and implemented in magnetic tunnel junctions (MTJs) [4,5]. However, the development of PMA in materials based on F/MO_x interfaces is still problematic due to incomplete understanding of its causes. Some researchers declare that PMA can be created only through a hybridization of F 3*d* and O 2*p* orbitals at the F/MO_x interface, while others show that placing an appropriate underlying nonmagnetic material is critical for developing PMA [6–10]. Studies of the electronic structures of F/MO_x linked together with magnetic measurements and theoretical studies should, hopefully, lead to a full understanding of PMA in such systems.

XPS is one of the primary tools used to analyze the interfaces utilizing either conventional X-ray tubes or complex synchrotron sources. These studies are frequently accompanied by sputtering to investigate depth dependence of XPS signals. That, however, may lead to unambiguous results due to the fact that an interpretation of XPS data for buried interfaces recorded in combination with ion sputtering procedure should be performed with special care as sputtering itself can seriously affect the interlayer structure [11]. One should remember that ion sputtering, even when using noble gas ions, generates a large number of artifacts in subsurface region, as for instance, atomic mixing and knock-on implantation, preferential sputtering, bond breaking, phase formation, segregation, radiation-enhanced diffusion, roughness formation, etc. Such effects have been studied over the last decades and critical reviews of their influences on surface analytical techniques were published [12–16]. Taking into account the knowledge gathered within experimental observation of electronic structure modification due to sputtering procedure, it was decided to abandon it and study potential electronic structure modification at Co/MgO interface after addition of the thin layer of Au without sputtering procedure.

The samples containing Co/MgO interface with and without a thin gold interlayer in-between were grown onto a-plane sapphire substrate at room temperature by molecular beam epitaxy (MBE). Complete

* Corresponding author.
E-mail address: demch@ifpan.edu.pl (I.N. Demchenko).

https://doi.org/10.1016/j.scriptamat.2017.10.006
1359-6462/

details of their growth procedure can be found in [6]. The thicknesses of each layer in the samples were identified as Mo(20 nm)/Au(20 nm)/Co(1.8 nm)/Au(0.3 nm)/MgO(2 nm) (Sample 1) and Mo(20 nm)/Au(20 nm)/Co(1.8 nm)/MgO(5 nm) (Sample 2).

Ferromagnetic resonance (FMR) measurements were performed at room temperature with a conventional X-band (f = 9.38 GHz) Bruker EMX spectrometer. A quartz rod was used as a sample holder and the FMR resonance field (H_{res}) was recorded as a function of the angle (θ_H) between the direction of the external magnetic field (H_{ext}) and normal to the sample's surface. In case of Sample 2 (with Co/MgO interface) a maximum ($\mu_0 H_{res} = 0.73$ T) and minimum ($\mu_0 H_{res} = 0.17$ T) of H_{res} were observed for perpendicular and parallel orientations of the external magnetic field, respectively. These values indicate an easy axis of magnetization in the plane of the magnetic layer, i.e. in-plane magnetic anisotropy (IMA), see Fig. 1(d). However, the structure with the gold incorporated at Co/MgO interface (Sample 1) has a maximum ($\mu_0 H_{res} = 0.41$ T) and minimum ($\mu_0 H_{res} = 0.13$ T) of H_{res} for parallel and perpendicular orientations of the H_{ext}, respectively: easy axis of magnetization is perpendicular to the plane now, see Fig. 1(c). A significant enhancement of the surface anisotropy energy of cobalt layer ($d_{Co} \sim 1.8$ nm) occurs due to insertion of a gold monolayer between Co and MgO, such that it overcomes the shape and magnetocrystalline magnetic anisotropy leading to PMA.

In order to understand the origins of this effect, the samples were studied by XPS using a Scienta/Prevac spectrometer system with monochromatic Al Kα radiation ($h\nu = 1486.6$ eV) from an X-ray source (ScientaVG, MX650) irradiating a spot size of 6×2 mm^2 while operating at 300 W. The high resolution (HR) XPS spectra were collected with the hemispherical analyzer (ScientaVG R4000) at two different take-off angles (0°, and 60° to the surface's normal) with a pass energy of 100 eV and an energy step size of 0.15 eV. Let us note that for the used spectrometer set-up the FWHM of Ag 3*d* line is about 0.6 eV. The slit of the analyzer has a curved shape with the dimension 0.5×25 mm^2 (width vs. length), whereas angular aperture had 2 mm diameter which sets the acceptance angle to ±7°. Only the surface of the reference sample (Co film) was cleaned from carbon contamination and native cobalt oxides using the Ar ion source (Prevac IS40E) at 0.8–1.4 kV. The incident angle of the Ar ion beam is 69° from sample normal and the sputter area was 10×10 mm^2. A charge compensation for the investigated multilayers was achieved using a low energy electron flood gun (at ~1.1–6.7 eV). Binding energies of the photoelectrons were calibrated using gold $4f_{7/2}$ line (84 eV). The CasaXPS software (version 2.3.17) [17] was used to evaluate the XPS data. Simulation of Electron Spectra for Surface Analysis (SESSA) software [18] was used to estimate thicknesses and composition of examined layers. The details of such analysis could be found in [16].

The HR XPS spectra for Sample 1 (with the gold interlayer) are shown in Fig. 1(a, b). As it was mentioned above, the Au $4f_{7/2}$ photopeak maximum, located at 84 eV, was taken for calibration of energy scale (see Fig. 1(a)). The Au $4f_{5/2}$ peak is overlapped with the Mg 2*s* states corresponding to various oxides of magnesium (marked as "3" and "4") with binding energies (BE) of 88.6 and 89.3 eV. The obtained values agree well with the data presented in the literature [19], in which the Mg 2*s* peak positions of $Mg(OH)_2$, $MgCO_3$, and MgO are listed at the energies 89.2 eV, 89.3 eV, and 88.6 eV, respectively. Motivated by the uniqueness of peak shapes and positions within Auger spectra, which is useful for both elemental identification and chemical state analyses, a detailed analysis of Auger Mg KLL line in conjunction with Mg 1*s* XPS peak was performed (XPS spectra in the BE ranges 300–360 and 1300–1310 eV are not shown here). So-called Auger parameters (α) that can be used without interference of surface charging were identified. For each of the samples two Auger parameters for magnesium were found to be 998.6 and 997.7 eV. According to [20] the estimated values represent MgO and $Mg(OH)_2$&$MgCO_3$ species, respectively. Consequently, the electronic states corresponding to the mentioned above species reflect interaction of originally pure MgO phase (in the top layer) with atmosphere and following carbon contamination. According to SESSA calculations the thicknesses of that sub-layer and the following MgO one are ~20 ± 2 Å. The estimated thickness agrees well with the nominal one predicted from the growth process.

As our interest focuses on the top Co/MgO interface let us discuss the results for Co 2*p* line represented in Fig. 1(b). The parameters of deconvolution of Co $2p_{3/2}$ lines for Samples 1 and 2 are summarized in Table 1. The presented in Fig. 1(b) data are background subtracted and normalized to the maximum of Co^0 $2p_{3/2}$ peak intensity for clarity. They are compared to metallic cobalt film (reference sample) before and after surface cleaning. On the pristine reference sample one can distinguish two distinctive components corresponding to the metallic cobalt (Co^0, BE of $2p_{3/2}$: 778.0 ± 0.15 eV) and cobalt monoxide (Co(II)O, BE of $2p_{3/2}$: 780.2 ± 0.15 eV). The observed 'chemical shift' is an effective indicator of the charge transfer between O 2*p* and Co 3*d* states. Furthermore, one observes an Auger peak (Co LMM: 777 ± 0.15 eV) and satellite structures (marked "S" in Fig. 1(b)) at higher binding energy for the reference sample before and after sputtering. An explanation of Co 2*p* XPS spectral shape of cobalt dihalides and CoO was developed in [21,22] taking into account the 3*d*-multiplet coupling and the covalency hybridization among $3d^7$, $3d^8\underline{L}$, and $3d^9\underline{L}^2$ configurations (here $\underline{L}$ denotes a hole in the ligand orbital). According to such interpretation,

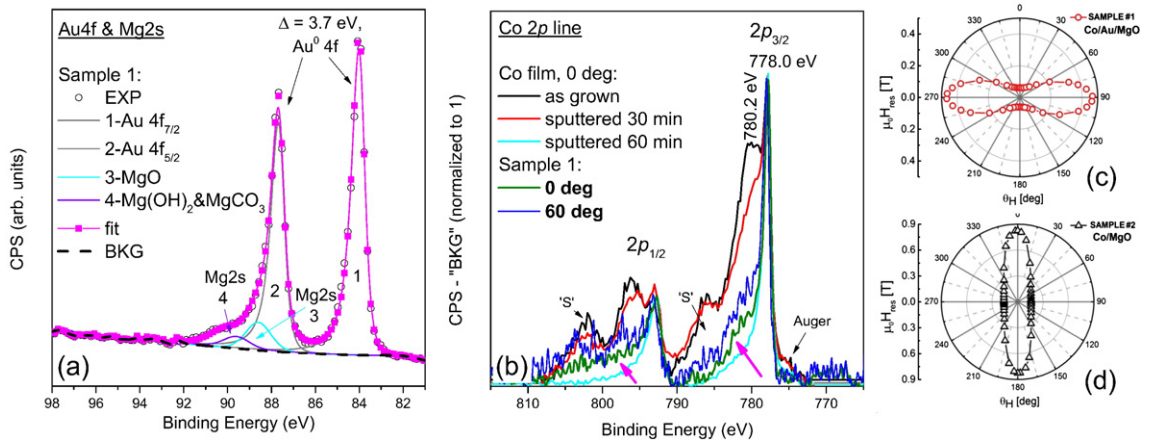

Fig. 1. XPS spectra for Sample 1 (Co/MgO interface with the gold interlayer): (a) split of Au 4*f* and Mg 2*s* states; (b) Co 2*p* states compared to metallic cobalt (after and before surface cleaning, see text for details); (c) Auger Mg KLL; (d) Mg 1*s* line. The polar angle dependence of the resonant field as a function of the angle between the direction of external magnetic field H_{ext}, and the normal to the sample surface for (c) Sample 1: Au(20 nm)/Co (1.8 nm)/Au(0.3 nm)/MgO(2 nm) and (d) Sample 2: Au(20 nm)/Co(1.8 nm)/MgO(5 nm).

Table 1
Cobalt $2p_{3/2}$ spectral fitting parameters for metallic cobalt, Sample 1, and Sample 2. The energy calibration was done for Au $4f_{7/2}$ line at 84 eV.

Components	Description	Position (eV) ± 0.15 eV	FWHM (eV)	L. Sh.	% Area	% St. Dev.
		Reference: Metallic cobalt - sputtered				
Co^O	Auger LMM	777.0	3.12	GL(30)	12.27	0.06
	$2p_{3/2}$	778.0	0.75	LA(1.2,5,5)	70.75	0.05
	Plasmon 1	781.0	3.28	GL(30)	9.91	0.01
	Plasmon 2	783.0	3.28	GL(30)	7.08	0.01
		Sample 1: Au/Co/Au(0.3 nm)/MgO				
Co^O	Auger LMM	777.0	3.12	GL(30)	10.80	0.07
	$2p_{3/2}$	778.0	0.75	LA(1.2,5,5)	64.86	0.15
	Plasmon 1	781.0	3.28	GL(30)	9.08	0.02
	Plasmon 2	783.0	3.28	GL(30)	6.49	0.02
Co(II)O	**$2p_{3/2}$**	779.9	2.3	GL(30)	4.38	0.07
	S 1	782.2	2.6	GL(30)	2.41	0.04
	S 2	786.4	3.7	GL(30)	1.97	0.09
		Sample 2: Au/Co/MgO				
Co^O	Auger LMM	776.94	3.12	GL(30)	7.7	0.16
	$2p_{3/2}$	777.94	0.75	LA(1.2,5,5)	58.05	0.21
	Plasmon 1	780.94	3.28	GL(30)	8.13	0.03
	Plasmon 2	782.94	3.28	GL(30)	5.80	0.02
Co(II)O	**$2p_{3/2}$**	779.84	2.3	GL(30)	10.16	0.08
	S 1	782.14	2.6	GL(30)	5.60	0.04
	S 2	786.34	3.7	GL(30)	4.57	0.04

the main peaks are ascribed to the $d^8\underline{L}$ final states and the satellite structure is a mixture of the d^7 and $d^9\underline{L}^2$ final states. Note also that multiplet splitting of $3d^7$ states in the $2p_{3/2}$ spectrum is so remarkable that its higher binding energy end almost reaches the $2p_{1/2}$ spectrum.

After 60 min of surface cleaning of the reference Co film the contribution of CoO disappears and pure metallic phase of cobalt with $2p$ spin-orbit splitting 14.97 eV is clearly observed (Fig. 1(b)). The observed asymmetric Co^0 peak shape of sputter-cleaned cobalt surface (cyan line in Fig. 1(b)) is due to the interaction of the emitted photoelectron with the conduction electrons available in conductive/metallic samples. These shake-up like events generate a tail on the higher binding energy side of the main peak instead of discrete shake-up satellites [23]. The comparison of the Co $2p$ states of Sample 1 to the reference sample (with a varied geometry of the XPS signal acquisition) manifests overlaying of minor cobalt oxide component with the major contribution of metallic cobalt. By deconvolution of the Co $2p_{3/2}$ peak, the fraction of Co(II) in Sample 1 is determined to be 9.8% [24]. This indicates that despite a thin gold interlayer between cobalt and magnesium oxide layers some amount of cobalt atoms is bonded to oxygen. This observation allowed us to suggest that gold layer grown on the cobalt top interface is in the form of non-coalescing islands, in other words, the top gold interlayer is not continuous. Thus, during deposition of the MgO layer, oxygen atoms from the MgO combine with the neighboring Co atoms, leading to a formation of CoO at the Co/MgO interface in areas between the gold islands. Estimated by SESSA software thickness of CoO at metallic cobalt interface is ~7 ± 2 Å.

Before general discussion of the influence of gold interlayer (between Co/MgO) on magnetic anisotropy of Sample 1 let us briefly present XPS the results concerning the sample without gold interlayer between cobalt and magnesium oxide layers. The obtained XPS results for Co $2p_{3/2}$ line are also listed in Table 1. The main conclusion is that the fraction of cobalt oxide phase in this sample is about two times larger compared to the sample with gold interlayer. That means that oxygen atoms from MgO combine with the neighboring Co atoms leading to a formation of CoO at the Co/MgO interface. Estimated by SESSA software thickness of CoO interlayer at metallic cobalt interface for that sample is bigger compared to Sample 1 and is equal to ~10 ± 2 Å.

The results previously published for Co/AlO_x system [10] strongly suggest that the onset of PMA is related to the appearance of a significant density of interfacial Co—O bondings at the Co/AlO_x interface. However, the here-investigated Au/Co/MgO structure (Sample 2) reveals larger fraction of cobalt oxide compared to the sample with gold interlayer between Co and MgO (Sample 1) but, at the same time, IMA instead of PMA is observed. Consequently, there should be another factor explaining such an effect. First principle calculations for Fe/MgO and Co/MgO systems presented in [9] make clear that in the case of ideal metal/isolator interfaces both systems reveal PMA with values of 2.93 and 0.38 erg/cm^2, respectively. That obviously differs for the investigated case since Sample 2 demonstrates IMA. The calculations for Fe/MgO showed that PMA weakens in the presence of interfacial disorder and lowers down to 2.27 and 0.98 erg/cm^2 for under- and over-oxidized cases, respectively [9]. The over-oxidation of metal layer is detrimental to PMA [25–27] because the number of mixed states with both metal d_z^2 and oxygen p_z orbitals (which is critical to PMA at "metal/nonmagnetic oxide" interface) *is reduced* due to the local charge redistribution induced by additional oxygen atoms (see Fig. 2 in [28] and its relevant discussion). This reduction is attributed to the split of the Co-d_z^2 and O-p_z hybridized states around Fermi level in the presence of an additional oxygen. As a surface energy is decreased, the IMA in Sample 2 is observed.

The origin of PMA in Sample 1 could be explained as follows. The fitted surface anisotropy constant K_S [6] for Au/Co/Au(0.3 nm)/MgO heterostructure is 1.6 erg/cm^2 (let us note that estimated value is higher than for Au/Co/MgO heterostructure (1.2 erg/cm^2)) and is approximately 4 times larger than theoretically predicted PMA value of 0.38 erg/cm^2 for ideal Co/MgO interface [9]. A decreased fraction of the cobalt monoxide (down to 9.8%) *and* an assumption of ideal Co/MgO interface do not explain fully the estimated value of K_s. A possible explanation (additional factor) of PMA existence in Sample 1 is the interfacial hybridization, i.e., a strong spin-orbit (SO) interaction, between the magnetic (cobalt) and nonmagnetic (gold) metals. For instance, several theoretical studies [29–32] predicted that large SO coupling of Pd plays an important role for obtaining PMA in Co/Pd multilayers. In fact, there are plenty reports regarding Co/Pd, Co/Pt, and Co/Au films possessing PMA [3,33,34]. All authors share the same opinion that a strong interfacial *d-d* hybridization produces an enhanced perpendicular Co orbital momentum, which causes PMA by SO coupling. Consequently, it is likely that *d-d* hybridization increases the surface energy (0.83 erg/cm^2 for Co/Au interface [6]) and plays an important role in developing PMA, as it appears for Sample 1. In other words, introduction of the gold interlayer at the Co/MgO interface induces the hybridization of Au 5*d* levels with 3*d* electrons of the ferromagnetic layer that generates/enhances PMA, in context of mixed states with both metal d_z^2 and oxygen p_z orbitals at Co/MgO interface.

The results of XPS analysis presented here show clearly that some fraction of Co atoms at the Co/MgO interface is bonded to oxygen atoms. Moreover, an "oxidation zone" (thickness of CoO interlayer estimated by SESSA software) is bigger for approximately 1.5 times for sample revealing IMA (Sample 1, without gold interlayer). With this in mind, the reaction of Co with oxygen atom through oxygen migration mechanism [11,35,36] can be attributed via the redox reaction at the Co/MgO interface. It is clear that in Sample 1 the non-continuous gold interlayer between Co/MgO partially blocks the migration of oxygen atoms into the layer of cobalt. The discussed above "over-oxidation" of the Co/MgO interface turns out to be the only reason to explain decreasing of a surface energy leading to IMA for the sample without gold interlayer (Sample 2). The opposite is true for the sample with the gold interlayer (Sample 1), namely, a metal-metal SO interaction plays a leading role in the manifestation of PMA. It is important to note also that according to [37] other effects like interface roughness, magnetostriction, etc., all are not considered here, may also come into play.

In summary, the Au 4*f*, Mg 2*s*, Mg 1*s*, and Co 2*p* HR XPS spectra along with Auger Mg KLL were probed for Au/Co/MgO and Au/Co/Au(0.3 nm)/MgO systems. The estimated by de-convolution of $2p_{3/2}$ XPS spectrum amount of CoO phase in Au/Co/MgO is approximately 22%. The split of the Co-d_z^2 and O-p_z hybridized states around Fermi level at the Co/MgO interface was predicted as result of the interface over-oxidation. The presence of an excess of oxygen atoms at the Co/MgO interface lowers the surface energy and the magnetization is in the sample plane. The analysis of Co $2p_{3/2}$ XPS line for Au/Co/Au(0.3 nm)/MgO structure indicates the presence of approximately 9.8% CoO phase (the thickness of this interlayer is approximately twice smaller compared to the sample without Au interlayer), as an effect of introduction of the Au interlayer preventing the Co against oxidation. Consequently, the *d*-*d* hybridization of Co and Au increases the surface anisotropy energy and ensures PMA is present for thin Co layer. The low fraction of CoO at the interface can only slightly reduce the surface energy value. Overall, the obtained results identify a possibility of controlling the type of magnetic anisotropy in Co/MgO systems through addition of a gold interlayer, the fact that could be used in novel devices for spintronics.

This work was partially supported by the EAgLE international project (FP7-REGPOT-2013-1, Project No. 316014) and the international project co-financed by Polish Ministry of Science and Higher Education, Grant Agreement 2819/7.PR/2013/2.

References

[1] [a] P.F. Carcia, A.D. Meinhaldt, A. Suna, Appl. Phys. Lett. 47 (1985) 178;
[b] H.J.G. Draaisma, F.J.A. den Broeder, W.J.M. de Jonge, J. Magn. Magn. Mater. 66 (1987) 351;
[c] F.J.A. den Broeder, D. Kuiper, A.P. van de Mosselaer, W. Hoving, Phys. Rev. Lett. 60 (1988) 2769.
[2] G.H.O. Daalderop, P.J. Kelly, M.F.H. Shuurmans, Phys. Rev. B 50 (1994) 9989.
[3] N. Nakajima, T. Koide, T. Shidara, H. Miyauchi, H. Fukutani, A. Fujimori, K. Iio, T. Katayama, M. Nyvlt, Y. Suzuki, Phys. Rev. Lett. 81 (1998) 5229.
[4] M. Mizuguchi, Y. Hamada, R. Matsumoto, S. Nishioka, H. Maehara, K. Tsunekawa, D.D. Djayaprawira, N. Watanabe, T. Nagahama, A. Fukushima, H. Kubota, S. Yuasa, M. Shiraishi, Y. Suzuki, J. Appl. Phys. 99 (2006), 08T309.
[5] S. Ikeda, J. Hayakawa, Y.M. Lee, F. Matsukura, Y. Ohno, T. Hanyu, H. Ohno, IEEE Trans. Electron Devices 54 (2007) 991.
[6] L. Gladczuk, P. Aleshkevych, K. Lasek, P. Przyslupski, J. Appl. Phys. 116 (2014) 233909.
[7] J.Y. Zhang, G. Yang, S.G. Wang, Y.W. Liu, Z.D. Zhao, Z.L. Wu, S.L. Zhang, X. Chen, C. Feng, G.H. Yu, J. Appl. Phys. 116 (2014) 163905.
[8] D. Chen, X.L. Ma, Y.M. Wang, Phys. Rev. B 75 (2007) 125409.
[9] H.X. Yang, M. Chshiev, B. Dieny, J.H. Lee, A. Manchon, K.H. Shin, Phys. Rev. B 84 (2011) 054401.
[10] A. Manchon, C. Ducruet, L. Lombard, S. Auffret, B. Rodmacq, B. Dieny, S. Pizzini, J. Vogel, V. Uhlíř, M. Hochstrasser, G. Panaccione, J. Appl. Phys. 104 (2008) 043914.
[11] X. Chen, C. Feng, Z.L. Wu, F. Yang, Y. Liu, S. Jiang, M.H. Li, G.H. Yu, Appl. Phys. Lett. 104 (2014) 052413.
[12] D. Briggs, M.P. Seah, Auger and X-ray Photoelectron Spectroscopy, 1, Wiley, Chichester, 1990.
[13] N.Q. Lam, Surf. Interface Anal. 12 (1988) 65.
[14] S. Hofmann, Rep. Prog. Phys. 61 (1998) 827.
[15] S. Oswald, R. Reiche, Appl. Surf. Sci. 179 (2001) 307.
[16] I.N. Demchenko, W. Lisowski, Y. Syryanyy, Y. Melikhov, I. Zaytseva, P. Konstantynov, M. Chernyshova, M.Z. Cieplak, Appl. Surf. Sci. 399 (2017) 32.
[17] Software package for the analysis of XPS results, CasaXPS version 2.3.17dev6.6o, see http://www.casaxps.com.
[18] W. Smekal, W.S.M. Werner, C.J. Powell, Surf. Interface Anal. 37 (2005) 1059.
[19] Handbooks of Monochromatic XPS Spectra. XPS International, Inc., 3408 Emerald Drive, Ames, Iowa, 50010 USA, 1999.
[20] Y. Bouvier, B. Mutel, J. Grimblot, Surf. Coat. Technol. 180–181 (2004) 169.
[21] Recent Advances in Magnetism of Transition Metal Compounds, Festschrift in Honour of Professor K MotizukiMar 1993 (Edited by: A Kotani (Univ. Tokyo), N Suzuki (Osaka Univ.) 392 pp., ISBN: 981-02-1150-3).
[22] F. de Groot, A. Kotani (Eds.), Core Level Spectroscopy of Solids (Advances in Condensed Matter Science), 1st editionCRC Press, March 10, 2008 (ISBN-13: 978-0849390715).
[23] D. Briggs, in: D. Briggs, J.T. Grant (Eds.), Surface Analysis by Auger and X-ray Photoelectron Spectroscopy, IM Publications, Chichester, 2003.
[24] Here, the CoO fraction is calculated as the ratio of CoO phase to the metallic cobalt phase in the cobalt layer. The amount of each phase was determined estimating areas of the respective photoelectron sub-peaks during de-convolution of XPS spectra normalized to 100%.
[25] D. Lacour, M. Hehn, M. Alnot, F. Montaigne, F. Greullet, G. Lengaigne, O. Lenoble, S. Robert, A. Schuhl, Appl. Phys. Lett. 90 (2007) 192506.
[26] A.J. Schellekens, L. Deen, D. Wang, J.T. Kohlhepp, H.J.M. Swagten, B. Koopmans, Appl. Phys. Lett. 102 (2013) 082405.
[27] K.H. Khoo, G. Wu, M.H. Jhon, M. Tran, F. Ernult, K. Eason, H.J. Choi, C.K. Gan, Phys. Rev. B 87 (2013) 174403.
[28] X.G. Zhang, W.H. Butler, A. Bandyopadhyay, Phys. Rev. B 68 (2003) 092402.
[29] J.G. Gay, R. Richter, Phys. Rev. Lett. 56 (1986) 2728.
[30] G.H.O. Daalderop, P.J. Kelly, den F.J.A. Broeder, Phys. Rev. Lett. 68 (1992) 682 (Phys. Rev. B 42 (1990) 7270; ibid. 50 (1994) 9989).
[31] D.S. Wang, et al., Phys. Rev. Lett. 70 (1993) 869 (Phys. Rev. B 48 (1993) 15 886; J. Magn. Magn. Mater. 129 (1994) 237).
[32] R. Wu, C. Lee, A.J. Freeman, J. Magn. Magn. Mater. 99 (1991) 71.
[33] P.F. Carcia, J. Appl. Phys. 63 (1988) 5066.
[34] B.N. Engel, C.D. England, R.A.V. Leeuwen, M.H. Wiedmann, C.M. Falco, Phys. Rev. Lett. 67 (1991) 1910.
[35] X. Zhou, Y. Yan, M. Jiang, B. Cui, F. Pan, C. Song, J. Phys. Chem. C 120 (2016) 1633.
[36] D.A. Gilbert, J. Olamit, R.K. Dumas, B.J. Kirby, A.J. Grutter, B.B. Maranville, E. Arenholz, J.A. Borchers, K. Liu, Nat. Commun. 7 (2016) 11050.
[37] L. Cagnon, T. Devolder, R. Cortes, A. Morrone, J.E. Schmidt, C. Chappert, P. Allongue, Phys. Rev. B 63 (2001) 104419.